Single-Crystal Elasticity of the α and β of Mg_2SiO_4 Polymorphs at High Pressure

Chang-Sheng Zha[1], Thomas S. Duffy[2], Robert T. Downs[1], Ho-kwang Mao[1], Russell J. Hemley[1,3], and Donald J. Weidner[4]

The full set of single-crystal elastic moduli of forsterite (α-Mg_2SiO_4) andwadsleyite (β-Mg_2SiO_4) were measured at pressures of 3-16 GPa and 0-14 GPa, respectively. For forsterite, the pressure derivatives of the bulk (K_0's) and shear (G_0') modulus are 4.2 ± 0.2 and 1.4 ± 0.1, respectively. For wadsleyite, the corresponding pressure derivatives are 4.3 ± 0.2 and 1.4 ± 0.2. These values are much lower than those reported in earlier, low-pressure studies for both materials. At the pressure of the 410-km seismic discontinuity, the room-temperature velocity increase across the α-β transition is 9.8% for compressional waves and 12.4% for shear waves. The results are consistent with an olivine fraction in the upper mantle of 30-50%.

INTRODUCTION

The elastic stiffness coefficients provide fundamental insight into the nature of atomic forces in solids. While the atomic structures of a vast range of substances have been explored at high pressure, the complete set of elastic stiffnesses are known only for a few, usually simple, materials. X ray diffraction experiments at high pressure can constrain the bulk modulus [e.g., *Knittle*, 1995], but these measurements typically provide no information on material response to shear deformation. Such information for Earth materials are critical for constraining mantle composition and structure. Knowledge of the individual elastic moduli are necessary for calculating acoustic wave velocities and their orientation dependence. Comparison of laboratory measurements of acoustic velocities with seismic velocities in the mantle has long been recognized as the most direct means to determine the mineralogy of the deep inaccessible regions of planetary interiors. Seismological studies employing stacking techniques are providing increasingly detailed models of impedance contrasts and velocity gradients in and near the mantle transition zone [*Shearer*, 1996]. In this region, the elastic moduli of the forsterite (α), wadsleyite (β), and spinel (γ) polymorphs of Mg_2SiO_4 are the most critical quantities. Phase equilibria data suggest that the seismic discontinuity near 410 km depth (about 13.8 GPa) is related to the α-β transformation in (Mg,Fe) $_2SiO_4$. The possible existence of a weaker discontinuity near 520 km depth (about 17.9 GPa) [*Shearer*, 1996] may be due to the β-γ transition. Elasticity data on the Mg_2SiO_4 polymorphs at high pressure place constraints

[1]Geophysical Laboratory and Center for High-Pressure Research, Carnegie Institution of Washington, 5251 Broad Branch Rd, NW, Washington, DC 20015

[2]Consortium for Advanced Radiation Sources, The University of Chicago, 5640 S. Ellis Ave, Chicago, IL 60637

[3]Also at: Laboratoire de Sciences de la Terre, Ecole Normale Superieure de Lyon, 69364 Lyon, France

[4]Department of Earth and Space Sciences and Center for High-Pressure Research, University at Stony Brook, Stony Brook, NY 11974 USA

Properties of Earth and Planetary Materials
at High Pressure and Temperature
Geophysical Monograph 101

on the total olivine fraction of the upper mantle at these depths [e.g., *Duffy et al.*, 1995].

Recently there have been a number of developments in experimental methods for acoustic velocity and elastic constant determination. At ambient pressure, there have been advances in resonant ultrasound spectroscopy [*Maynard,* 1996] and in direct imaging of acoustic velocity surfaces [*Wolfe and Hauser*, 1995]. There has also been considerable progress in the study of sound velocity and elasticity at high pressure. In the diamond anvil cell, Brillouin scattering [*Shimizu and Sasaki*, 1992; *Zha et al.*, 1993] and impulsive stimulated scattering [*Zaug et al.*, 1993] have been used to obtain single-crystal elastic constants to pressure as high as 24 GPa. Ultrasonic sound velocity measurements in the large volume press have been pioneered recently using both single crystals to 6 GPa [*Yoneda and Morioka,* 1992] and polycrystals to 12 GPa [*Li et al.*, 1996]. A recently developed gigahertz ultrasonic interferometer has also been used with the large volume press [*Chen et al.*, 1996] to obtain selected single-crystal constants at simultaneous high pressure and temperature.

EXPERIMENTAL TECHNIQUE

Brillouin scattering is the interaction of light (photons) with thermally excited long-wavelength lattice vibrations (phonons) in a crystal. Propagating acoustic waves produce fluctuations in the refractive index from which light is scattered. Since the fluctuations are moving at the acoustic velocity, the scattered light is shifted in frequency by the Doppler effect. Brillouin spectroscopy is similar to the more familiar Raman spectroscopy except that the frequency shifts in Brillouin scattering are very small (~1-2 cm^{-1}) and the signal intensity is weaker. The experimental challenge is to extract the weak Brillouin signal from the intense, elastically scattered light.

The geometry for Brillouin scattering in the diamond cell is shown in Figure 1. Light from a frequency-stabilized Ar laser is directed into the sample through one of the diamond anvils. The scattered radiation passes through the other anvil in a symmetric arrangement. A diamond anvil cell with a short piston-cylinder and a large optical opening was used in these experiments. The Brillouin scattered light is collected, spatially filtered, and passed through a tandem Fabry-Perot interferometer which eliminates overlap of successive interference orders. The frequency spectrum is recorded with a multichannel scaler. Further experimental details can be found in *Zha et al.* [1993; 1996].

In the platelet scattering geometry, light enters through one sample face and exits through another parallel face (Figure 1). The acoustic wave propagation direction is then perpendicular to the axis of the cell and coplanar with incident and scattered light. The equation relating the acoustic velocity, V, to the measured frequency shift, $\delta\nu$, for this geometry is

$$V = \delta\nu\, \lambda_0\, (2 \sin\theta)^{-1} \qquad (1)$$

where λ_0 is the incident laser wavelength, and θ is the angle between incident or scattered light and the diamond cell axis at the outer diamond surface. The refractive index is not needed to determine the velocity in this case. By rotating the diamond cell around its axis, the acoustic velocity distribution within the sample plane can be completely characterized.

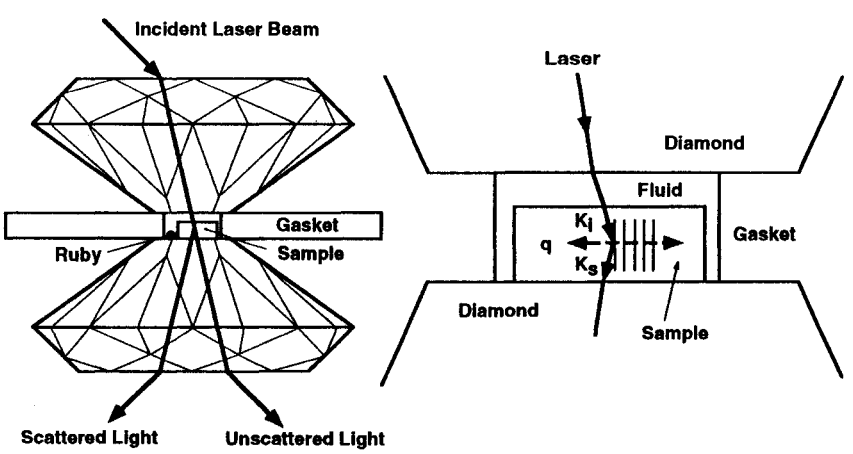

Figure 1. Brillouin scattering in the diamond anvil cell. Wavevectors for the incident photon (k_i), scattered photon (k_S), and phonon (q) are shown at the right. In the platelet geometry, light enters and exits the sample from opposite, parallel faces, and the acoustic wave propagates in the plane of the sample.

Single-crystal samples of Mg_2SiO_4 in the forsterite (α) and wadsleyite (β) structures were examined in this study. Electron microprobe analysis confirmed that both samples were pure end-members. For β-Mg_2SiO_4, electron microscopy also revealed the presence of submicron inclusions. No peaks attributable to hydroxyl bonds were observed by Raman spectroscopy. Several pieces of each material were polished to flat, parallel plates. Sample thicknesses ranged from 18 to 50 μm. The samples were oriented such that the polished plane intersected the three crystal axes at equal angles (within a few degrees). X ray diffraction was performed on both materials at ambient and selected high pressures. For forsterite, the cell volume determined by single-crystal X ray diffraction at ambient pressure was 290.22(9) Å^3, while for wadsleyite, the volume was 535.8(2) Å^3. These are consistent with previously reported values [*Smyth and McCormick*, 1995].

At low pressures, argon was used as a pressure transmitting medium. A 4:1 mixture of methanol-ethanol was used at intermediate pressures, and helium was the medium at the highest pressures. The choice of pressure medium was dictated by the need to establish nearly hydrostatic pressure conditions within the cell and to avoid overlap of Brillouin peaks from the sample and the pressure medium. At high pressures, it was found that the Brillouin peaks of the wadsleyite sample nearly overlapped the shear wave peaks from the diamond anvils. Since the volume of diamond is much larger than the sample volume, the Brillouin signal from the diamond can overwhelm the weaker sample signal. To overcome this problem, it was necessary to improve the spatial filtering by inserting cylindrical lenses in front and back of the cell to correct the astigmatic aberration introduced by the inclined positioned diamond cell. This was successful in reducing the intensity of the diamond peak by more than 90% for a 30-μm thick sample. It was sufficient to allow the sample Brillouin peaks to be measured over the pressure range studied here.

RESULTS

Sound velocities were generally measured at 10° intervals in the platelet plane at each pressure for both samples. In each direction, three acoustic velocities were determined: one quasi-longitudinal and two quasi-transverse. Figure 2 shows the complete set of acoustic velocities for wadsleyite in different loadings. A total of 144 directions and 400 individual acoustic velocities was measured. The average data collection time for a single direction is about 3 hours (but can vary considerably), so roughly a total data collection time of about 18 days (432 hours) was required. A comparable number of measurements was carried out on the forsterite sample.

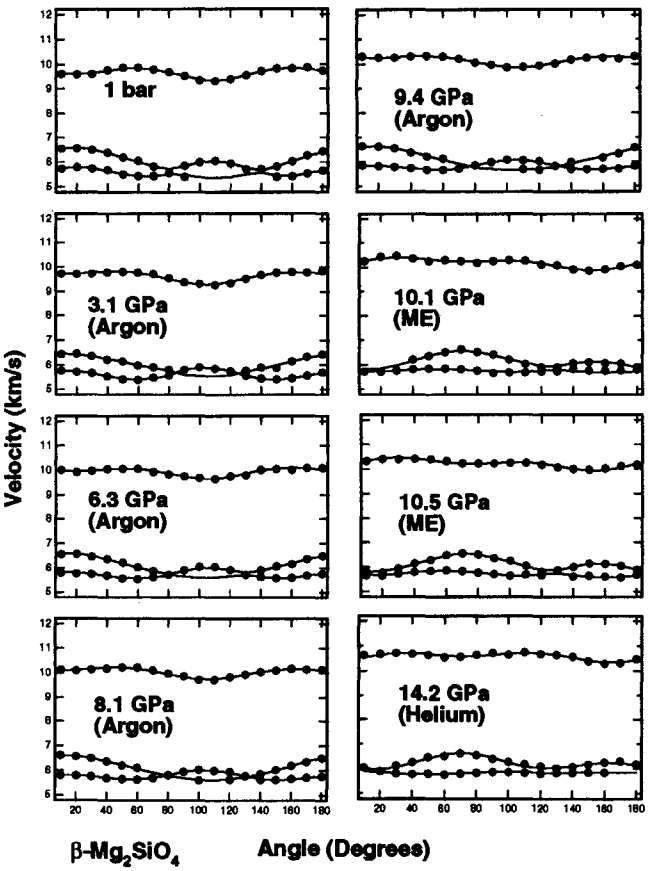

Figure 2. Acoustic velocity measurements for β-Mg_2SiO_4 The symbols are the experimental data and the solid lines are calculated using the best fitting elastic constants. The pressure and pressure-transmitting medium are indicated in each panel. The 10.1, 10.5 and 14.2 GPa are measured from second sample with different orientations. The angle is relative to an arbitrary marking on the cell. ME - 4:1 methanol-ethanol mixture.

The propagation of acoustic waves in anisotropic solids is governed by Christoffel's equation [*Auld*, 1973]. Using Cardan's solution of the cubic equations, this can be written as follows [*Rokhlin and Wang*, 1992]:

$$\rho V_j^2 = -a/3 + 2\sqrt{\frac{-p}{3}}\cos\left(\frac{\psi + 2\pi j}{3}\right), j = 0, 1, 2, \quad (2)$$

where ρ is the density, V_j are the acoustic velocities, and the other parameters are

$$\psi = \arccos\{-q/[2(p/3)]^{3/2}\}, \quad (3)$$

$$p = a^2/3 - b, \quad (4)$$

$$q = c - ab/3 + 2(a/3)^3, \quad (5)$$

$$a = - G_{ii}, \quad (6)$$

$$b = -(G^2_{12} + G^2_{13} + G^2_{23} - G_{11}G_{22} - G_{11}G_{33} - G_{22}G_{33}) \quad (7)$$

$$c = -(G_{11}G_{22}G_{33} + 2G_{12}G_{13}G_{23} - G_{11}G^2_{23} - G_{22}G^2_{13} - G_{33}G^2_{12}), \quad (8)$$

$$G_{im} = C_{ijlm}\, n_j n_l, \quad (9)$$

Summation over repeated indices is implied; $\xrightarrow[n]{}$[vectors n_1, n_2, n_3...] specifies the acoustic wave propagation direction. C_{ijlm} is the tensor of elastic constants which can also be written in the contracted Voigt notation, Cij, where i,j = 1,2,...,6 [*Nye*, 1985]. Both forsterite and wadsleyite are of orthorhombic symmetry and are thus characterized by nine independent elastic moduli. Three of these (C_{11}, C_{22}, and C_{33}) are the longitudinal elastic moduli, C_{44}, C_{55}, C_{66} are the shear elastic moduli, and the remaining three (C_{12}, C_{13}, and C_{23}) are the off-diagonal moduli.

The acoustic velocity data were inverted using Equation (2) by nonlinear least squares to yield the elastic stiffness coefficients and three Eulerian angles which relate the laboratory and crystallographic reference frames [*Shimizu and Sasaki*, 1992; *Zha et al.*, 1996]. Acoustic velocity distributions for the best fitting elasticity and orientation parameters are shown by the solid curves in Figure 2 for

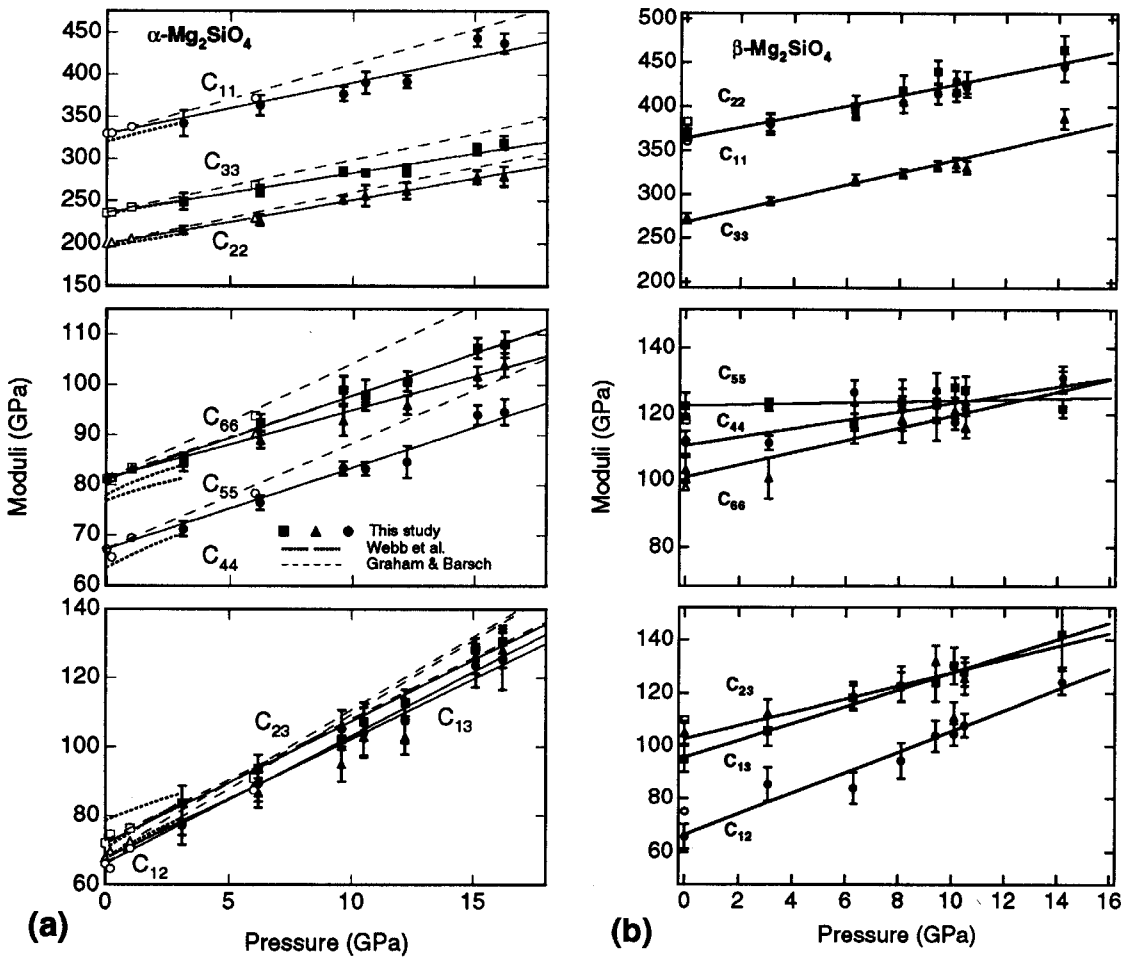

Figure 3. Elastic moduli as a function of pressure for (a) α-Mg_2SiO_4 and (b) β-Mg_2SiO_4. The filled symbols with error bars (2σ) are the present data points, and the solid lines are weighted least squares fits to the data. In (b), ambient pressure data of *Sawamoto et al.* [1984] are shown as open symbols. In (a), the dashed lines show extrapolation of 1-GPa results of *Graham and Barsch* [1969]. The doted lines show the results of *Webb* [1989]. In the middle panel, the curve for C_{55} of *Graham and Barsch* overlays that of C_{66} from this study. Ambient pressure data of *Isaak et al.* [1989] were used in determining the least squares fits.

wadsleyite. The root-mean-square deviation between measured and calculated acoustic velocities ranges from 20 m/s at 8.1 GPa to 42 m/s at 14.2 GPa. For forsterite, the RMS deviations were between 24 and 56 m/s [*Zha et al.*, 1996].

The pressure dependence of the elastic moduli of forsterite and wadsleyite is shown in Figures 3a and b. In all cases, a linear dependence of the moduli on pressure is obtained within the resolution of the data. For wadsleyite, the ambient pressure results of *Sawamoto et al.* [1984] are shown for comparison. Table 1 shows all elastic constants at different pressures for wadsleyite. There are no other single-crystal elasticity data at high pressure of which we are aware for this material. For forsterite, the present results are compared with extrapolations of previous single-crystal ultrasonic elasticity data to 1 GPa [*Graham and Barsch*, 1969]. For all the individual moduli, our measured values lie significantly below the values extrapolated from low-pressure.

Established velocity averaging techniques (Voigt-Reuss-Hill) were used to compute bounds on the elastic properties of a randomly oriented polycrystalline aggregate from the single-crystal properties. The resulting bulk and shear moduli for the two polymorphs are shown in Figure 4. Values for the aggregate moduli and their pressure derivatives were determined by fitting the experimental data to finite strain expressions for the bulk and shear moduli [*Davies*, 1974; *Davies and Dziewonski*, 1975] (Table 2). For forsterite, the pressure derivatives of the bulk and shear modulus are much lower than those found in early, low-pressure ultrasonic studies which reported pressure derivatives of the bulk modulus between 5.0 and 5.4, and pressure derivatives of the shear modulus of 1.8 [*Kumazawa and Anderson,* 1969; *Graham and Barsch*, 1969]. More recent high-pressure ultrasonic studies of forsterite single-crystals [*Yoneda and Morioka*, 1992] and polycrystalline aggregates [*Li et al.*, 1996] in the large-volume press give results consistent with ours. Recent work on a forsterite sample containing 10 mol% Fe using the impulsive stimulated scattering technique [*Zaug et al.*, 1993] is also generally consistent with the results reported here, except that no nonlinear behavior of the shear modulus is observed in our study of the iron-free end-member.

For wadsleyite, our ambient-pressure aggregate elastic moduli (Table 2) are comparable to those reported by *Sawamoto et al.* [1984] (K_0 = 174 GPa, G_0 = 114 GPa). Pressure derivatives for this material were first reported by *Gwanmesia et al.* [1990] from measurements on poly-

TABLE 1. Elastic Moduli of Wadsleyite (all in GPa)

P	C_{11}	C_{22}	C_{33}	C_{44}	C_{55}	C_{66}	C_{12}	C_{13}	C_{23}
0.0	370.47	367.74	272.43	111.20	122.48	103.05	65.59	95.20	105.14
	±7.84	±6.50	±5.82	±3.58	±4.00	±3.86	±4.54	±5.18	±4.36
3.1	379.28	382.01	292.21	111.24	122.71	100.70	85.39	105.53	112.39
	±11.46	±10.40	±4.46	±2.16	±1.84	±6.10	±6.62	±5.44	±5.28
6.3	393.35	399.90	316.69	126.59	117.53	116.96	83.91	118.23	119.10
	±7.90	±12.30	±6.06	±3.68	±2.58	±5.76	±6.14	±4.62	±4.98
8.1	404.22	418.33	323.99	121.37	123.58	118.46	94.42	122.31	123.37
	±11.22	±16.78	±5.42	±6.36	±6.74	±6.98	±6.82	±5.48	±6.70
9.4	414.42	439.78	333.08	127.13	122.77	118.43	103.89	123.78	131.81
	±11.16	±13.04	±5.76	±5.32	±3.80	±6.40	±5.90	±6.80	±5.92
10.1	428.83	415.97	333.91	117.55	128.19	121.09	104.48	130.21	110.77
	±11.30	±9.86	±7.90	±2.22	±3.08	±2.40	±4.10	±6.90	±5.80
10.5	421.89	425.66	330.73	121.65	127.21	116.16	107.78	127.90	125.39
	±6.72	±14.22	±7.70	±6.76	±4.32	±3.32	±4.38	±5.42	±5.98
14.2	444.47	464.89	386.83	130.94	121.67	129.71	123.93	141.95	151.85
	±15.86	±16.13	±11.30	±3.72	±2.76	±3.30	±4.56	±12.18	±19.60

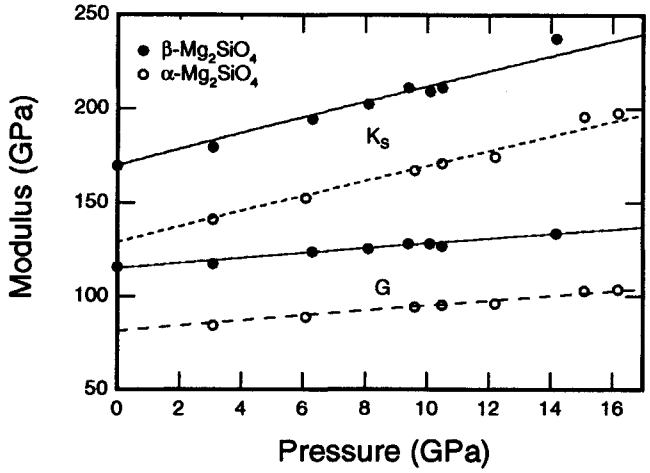

Figure 4. Bulk and shear moduli of α-Mg_2SiO_4 (open symbols) and β-Mg_2SiO_4(filled symbols). Lines are third order finite strain fits to the experimental data. Ambient pressure data of *Isaak et al.* [1989] were used in fitting the α-Mg_2SiO_4 data.

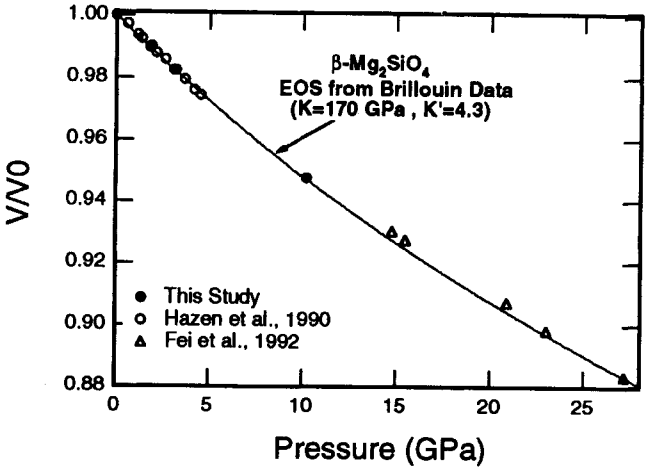

Figure 5. Compression data for β-$(Mg,Fe)_2SiO_4$. The data *of Fei et al.* [1992] were for a sample containing 16 mol% Fe; other data are for β-Mg_2SiO_4. The solid curve is a third-order equation of state from the present Brillouin data.

crystalline aggregates to 3 GPa. The values obtained in that study (K_0' = 4.8±0.1 and G_0' = 1.8±0.1) are considerably higher than those obtained here. Very recently, *Li et al.* [1996] using a similar approach to *Gwanmesia et al.* have measured pressure derivatives of β-Mg_2SiO_4 to 12 GPa. When fit to finite strain expressions, the resulting pressure derivatives (K_0' = 4.5 and G_0' = 1.6) are intermediate between our single-crystal results and the work of *Gwanmesia et al.* [1990]. The use of polycrystalline samples, which retain some porosity even at very high pressure, may be responsible for the higher pressure derivatives obtained in those studies.

A pressure-volume equation of state can be constructed from the Brillouin data by correcting the bulk modulus and its pressure derivatives from adiabatic to isothermal conditions. The correction is small and can be reliably estimated. Figure 5 compares the Brillouin equation of state for wadsleyite to X ray diffraction data from this and other studies. The good agreement obtained demonstrates the self-consistency of our results in that the densities predicted by our data are nearly identical to those used in the solution of Equation (2) above. Similar results were obtained for the forsterite samples [*Downs et al.*, 1996; *Zha et al.*, 1996].

TABLE 2. Aggregate Elastic Properties of Mg_2SiO_4 Polymorphs

Property	α-Mg_2SiO_4	β-Mg_2SiO_4
K_{0S} (GPa)	129[a]	170 (2)
G_0 (GPa)	79 [a]	115 (2)
K'_{0S}	4.2 (2)	4.3 (2)
G'_0	1.4 (1)	1.4 (2)

[a] *Isaak et al.* [1989]

DISCUSSION

This is the first study in which the elasticity of both the α and β polymorphs of Mg_2SiO_4 has been measured at pressures greater than that of the 410-km discontinuity in the mantle. Our primary finding is that the pressure dependencies of the aggregate moduli are nearly the same for both phases. This is consistent with values used in some earlier studies (e.g., *Duffy and Anderson*, 1989; *Gwanmesia et al.*, 1990), but the magnitudes of the derivatives are much lower than previously believed. Aggregate compressional and shear wave velocities are shown as a function of pressure in Figure 6. The velocity contrast between the α and β polymorphs is 12.3% and 14.2% at ambient pressure for compressional (P) and shear (S) waves, respectively, and decreases to 9.8% for P-waves and 12.4% for S-waves at the pressure of the 410-km discontinuity (~ 13.8 GPa). In comparison, the velocity seismic contrast across the discontinuity is 4-5%, although a recent study using stacks of long period records obtained an S-velocity jump at the discontinuity of only 3.4% [*Shearer*, 1996].

Figure 7 compares calculated sound velocities in the $(Mg,Fe)_2SiO_4$ polymorphs at high temperature to seismic velocity profiles for the upper mantle. The high-temperature mineral velocities were calculated along a 1600-K adiabat using the method of *Duffy et al.* [1995].

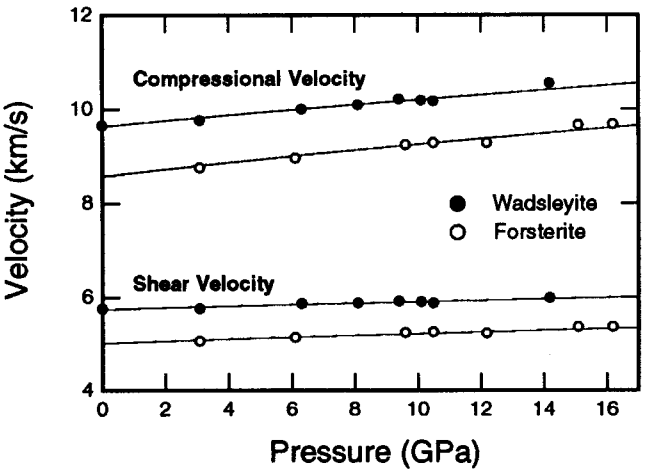

Figure 6. Aggregate compressional and shear velocity of wadsleyite and forsterite. Open and filled symbols are experimental data, solid lines are third-order finite strain fits to the data.

The only difference in this calculation is that our new measured values of the aggregate elastic properties of the β-phase have been used. The major uncertainty in calculating the high-temperature sound velocities is that the temperature derivative of the shear modulus ($\partial G/\partial T$) of β-Mg_2SiO_4 is unknown. Following *Duffy et al.* [1995], we adopt a range of values for this parameter between -0.014 GPa/K and -0.024 GPa/K, based on an evaluation of systematic trends in the larger mineral elasticity database. The lower estimate of the magnitude of the $\partial G/\partial T$ would be appropriate if the shear modulus temperature sensitivities of the α and β phases are the same. The larger value holds if the shear modulus of the β-phase is more sensitive to temperature than typical silicates are and has a value comparable to MgO and Al_2O_3.

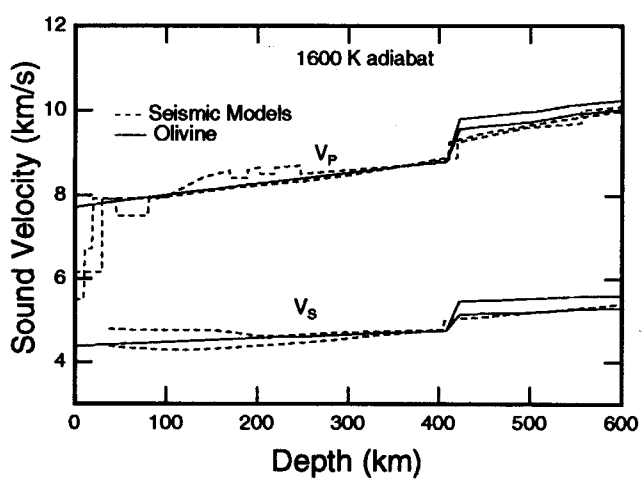

Figure 7. Acoustic velocities in the α-, β-, and γ- phases of $(Mg_{0.9},Fe_{0.1})_2SiO_4$ along a 1600-K adiabat (solid lines) compared with seismic velocity profiles for the upper mantle (dashed lines). The lower solid curve (at depths > 410 km) is for $\partial G/\partial T$ = -0.024 GPa/K. The upper solid curve is for $\partial G/\partial T$ = -0.014 GPa/K. The seismic models are from *Grand and Helmberger* [1984], *Walck et al.* [1984], and *Mechie et al.* [1993].

In the case of the lower temperature sensitivity, the velocity increase at 410 km under mantle conditions is consistent with olivine fractions of 30% (for shear waves) and 40% (for compressional waves) (Figure 7). Using the higher value for the shear modulus temperature sensitivity of β-Mg_2SiO_4, the amount of olivine consistent with the seismic discontinuity becomes 50% and 51% for compressional and shear waves, respectively. These values are slightly larger than those obtained by *Duffy et al.* [1995] because the pressure dependence of the aggregate elastic moduli of β-Mg_2SiO_4 measured here is lower than the values reported in the earlier work of *Gwanmesia et al.* [1990]. Note that the comparison with the recent long-period sdudy of *Shearer* [1996] would reduce the olivine content contributing at this depth.

Acknowledgments. We thank H. Yoder for providing the forsterite specimen and R. Liebermann and B. Li for providing preprints of papers. This work was supported by the Center for High Pressuer Research, National Science Foundation subcontract No. 431-3860A.

REFERENCES

Auld, B. A., *Acoustic Waves and Fields in Solids*, vol. 1, Wiley, New York, 1973.

Chen, G., H. A. Spetzler, I. C. Getting, and A. Yoneda, Selected elastic moduli and their temperature derivatives for olivine and garnet with different Mg/(Mg+Fe) contents - results from GHZ ultrasonic interferometry, *Geophys. Res. Lett., 23*, 5-8, 1996.

Davies, G. F., Effective elastic moduli under hydrostatic stress - 1. Quasi-harmonic theory, *J. Phys. Chem. Solids, 35*, 1513-1520, 1974.

Davies, G. F., and A. M. Dziewonski, Homogeneity and constitution of the Earth's lower mantle and outer core, *Phys. Earth Planet. Inter., 10*, 336-343, 1975.

Downs, R. T., C. S. Zha, T. S. Duffy, and L. W. Finger, The equation of state of forsterite to 17.2 GPa and effects of pressure media, *Am. Mineral., 81*, 51-55, 1996.

Duffy, T. S., and D. L. Anderson, Seismic velocities in mantle minerals and the mineralogy of the upper mantle, *J. Geophys. Res., 94*, 1895-1912, 1989.

Duffy, T. S., C. S. Zha, R. T. Downs, H. K. Mao, and R. J. Hemley, Elasticity of forsterite to 16 GPa and the composition of the upper mantle, *Nature, 378*, 170-173, 1995.

Fei, Y., H. K. Mao, J. Shu, G. Parthasarathy, and W. A. Bassett, Simultaneous high-P, high-T X ray diffraction study of β-$(Mg,Fe)_2SiO_4$ to 26 GPa and 900 K, *J. Geophys. Res., 97*, 4489-4495, 1992.

Graham, E. K., and G. R. Barsch, Elastic constants of single-crystal forsterite as a function of temperature and pressure, *J. Geophys. Res.*, *74*, 5949-5959, 1969.

Grand, S. P., and D. V. Helmberger, Upper mantle shear structure of North America, *Geophys. J. R. astr. Soc.*, *76*, 399-438, 1984.

Gwanmesia, G. D., S. Rigden, I. Jackson, and R. C. Liebermann, Pressure dependence of elastic wave velocity in β-Mg_2SiO_4 and the composition of the Earth's mantle, *Science*, *250*, 794-797, 1990.

Hazen, R. M., J. Zhang, and J. Ko, Effects of Fe/Mg on the compressibility of synthetic wadsleyite: β-$(Mg_{1-x}Fe_x)_2SiO_4$ ($x \approx 0.25$), *Phys. Chem. Minerals*, *17*, 416-419, 1990.

Isaak, D. G., O. L. Anderson, T. Goto, and I. Suzuki, Elasticity of single-crystal forsterite measured to 1700 K, *J. Geophys. Res.*, *94*, 5895-5906, 1989.

Knittle, E., Static compression measurements of equations of state, in *Mineral Physics and Crystallography: A Handbook of Physical Constants*, edited by T. J. Ahrens, pp. 98-142, AGU, Washington D. C., 1995.

Kumazawa, M., and O. L. Anderson, Elastic moduli, pressure derivatives, and temperature derivatives of single-crystal olivine and single-crystal forsterite, *J. Geophys. Res.*, *74*, 5961-5972, 1969.

Li, B., G. D. Gwanmesia, and R. C. Liebermann, Sound velocities of olivine and beta polymorphs of Mg_2SiO_4 at Earth's transition zone pressures, *Geophys. Res. Lett.*, *23*, 2259-2262, 1996.

Maynard, J., Resonant ultrasound spectroscopy, *Physics Today*, 26-31, Jan. 1996.

Mechie, J., A. V. Egorkin, K. Fuchs, T. Ryberg, L. Solodilov, and F. Wenzel, P-wave mantle velocity structure beneath northern Eurasia from long-range recordings along profile quartz, *Phys. Earth Planet. Int.*, *79*, 269-186, 1993.

Nye, J. F., *Physical Properties of Crystals*, Oxford Press, Oxford, 1985.

Rokhlin, S. I., and W. Wang, Double through-transmission bulk wave method for ultrasonic phase velocity measurement and determination of elastic constants of composite materials, *J. Acoust. Soc. Am.*, *91*, 3303-3312, 1992.

Sawamoto, H., D. J. Weidner, S. Sasaki, and M. Kumazawa, single-crystal elastic properties of the modified spinel (Beta) phase of magnesium orthosilicate, *Science*, *224*, 749-751, 1984.

Shearer, P. M., Transition zone velocity gradients and the 520-km discontinuity, *J. Geophys. Res.*, *101*, 3053-3066, 1996.

Shimizu, H., and S. Sasaki, High-pressure Brillouin studies and elastic properties of single-crystal H_2S grown in a diamond cell, *Science*, *257*, 514-516, 1992.

Smyth, J. R., and T. C. McCormick, Crystallographic data for minerals, in *Mineral Physics and Crystallography: A Handbook of Physical Constants*, edited by T. J. Ahrens, pp.1-17, AGU, Washington D. C., 1995.

Walck, M. C., The P-wave upper mantle structure beneath an active spreading center: The Gulf of California, *Geophys. J. r. astro. Soc.*, *76*, 697-723, 1984.

Webb S. L., The elasticity of the upper mantle orthosilicates olivine and garnet to 3 GPa, *Phys Chem Minerals*, *16*, 684-692, 1989.

Wolfe, J. P., and M. R. Hauser, Acoustic wavefront imaging, *Ann. Physik*, *4*, 99-126, 1995.

Yoneda, A., and M. Morioka, Pressure derivatives of elastic constants of single crystal forsterite, in *High-Pressure Research: Application to Earth and Planetary Sciences*, *Geophys. Monogr. Ser.*, vol. 67, edited by Y. Syono and M. H. Manghnani, pp. 207-214, Terra Scientific, Tokyo/AGU, Washington, D. C., 1992.

Zaug, J. M., E. H. Abramson, J. M. Brown, and L. J. Slutsky, Sound velocities in olivine at Earth mantle pressures, *Science*, *260*, 1487-1489, 1993.

Zha, C. S., T. S. Duffy, H. K. Mao, and R. J. Hemley, Elasticity of hydrogen to 24 GPa from single-crystal Brillouin scattering and synchrotron x-ray diffraction, *Phys. Rev. B*, *48*, 9246-9255, 1993.

Zha, C. S., T. S. Duffy, R. T. Downs, H. K. Mao, and R. J. Hemley, Sound velocity and elasticity of single-crystal forsterite to 16 GPa, *J. Geophys. Res.*, *101*, B8, 17535-17545, 1996.

Robert T. Downs, Geophysical Laboratory and Center for High-Pressure Research, Carnegie Institution of Washington, 5251 Broad Branch Rd., NW, Washington, DC 20015.

Thomas S. Duffy and Russell J. Hemley, Consortium for Advanced Radiation Sources, The University of Chicago, 5640 S. Ellis Ave., Chicago, IL 60637.

Russell J. Hemley, also at: Laboratoire de Sciences de la Terre, Ecole Normale Superieure de Lyon, 69364 Lyon, France.

Ho-kwang Mao, Geophysical Laboratory and Center for High-Pressure Research, Carnegie Institution of Washington, 5251 Broad Branch Rd., NW, Washington, DC 20015.

Donald J. Weidner, Department of Earth and Space Sciences and Center for High-Pressure Research, State University of New York at Stony Brook, Stony Brook, NY 11974.

Chang-Sheng Zha, Geophysical Laboratory and Center for High-Pressure Research, Carnegie Institution of Washington, 5251 Broad Branch Rd., NW, Washington, DC 20015.